SOLPS-ITER SIMULATIONS OF AN X-POINT RADIATOR IN THE DIII-D HIGH-BETA HYBRID PLASMAS

X. MA[1], H. Q. WANG[1], Z. LI[1], A.W. LEONARD[1], D.M. THOMAS[1], R. MAURIZIO[1], F. SCOTTI[2]
[1]General Atomics
[2]Lawrence Livermore National Laboratory
Email: maxinxing@fusion.gat.com

DIII-D experiments have achieved promising core-edge integrated scenario plasmas which integrate high-beta hybrid core with completely detached divertors by leveraging the X-point radiator (XPR) divertor operation. For the first time in DIII-D, SOLPS-ITER modeling with full drifts is able to qualitatively reproduce the experimental measured plasma conditions with an XPR in the high-beta hybrid plasmas. It highlights the key role of neutrals, divertor closure and efficient pumping in the formation of an XPR and the effects of drifts on the distribution of plasma and radiation near the X-point.

Studies in ASDEX Upgrade (AUG) and JET found that this XPR, with a stable, localized and highly radiative phenomenon near the X-point inside the confined plasma, leads to a dissipated power fraction of 90%, mitigated ELMs and a fully detached divertor with a moderated confinement degradation, which is attractive for solving the power exhaust issue for tokamak reactors [1]. In DIII-D, the XPR operation has been achieved, coupled with a high-beta hybrid core. As shown in figure 1, with increased N_2 seeding rate, the divertor plasma evolves from attached state to partial detachment and eventually to complete detachment with an XPR. The radiation peak moves from the inner leg region outside the X-point, to the outer separatrix region above the X-point. For the high beta hybrid plasmas, shallow XPR with complete divertor detachment and high confinement high-beta (β_N ~3.0, H_{98}~1.25) have been simultaneously achieved using the ITER-similar shape. However, this plasma remains ELMing with giant ELMs leading to ~10% pedestal energy loss. With stronger N_2 puffing, the plasmas exhibit a deep XPR regime with 2x core radiation peaking at the pedestal, the ELMs are strongly mitigated, and the confinement is significantly reduced to H_{98}<1.0.

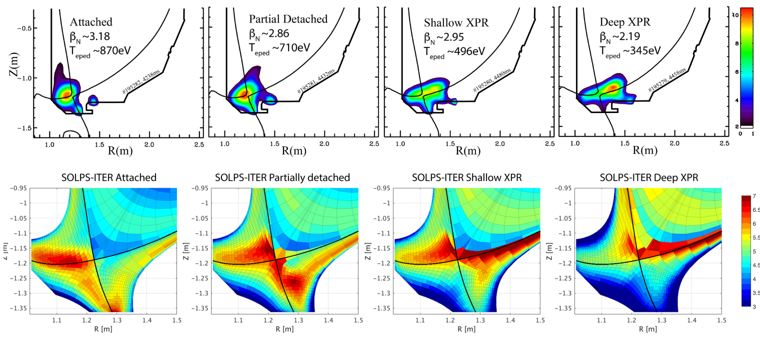

Fig. 1. *Top: 2D radiation reconstructions of bolometer measurements indicate the change of radiation pattern towards XPR with increased N_2 seeding rate. Bottom: Evolution of the total radiation (P_{rad}) pattern extracted from SOLPS-ITER modeling with increased N_2 seeding rate. From left to right, the impurity seeding is set to* 1×10^{20}/s, 4.3×10^{20}/s, 5.1×10^{20}/s *and* 5.4×10^{20}/s, *respectively.*

SOLPS-ITER code with kinetic neutral model EIRENE is used to understand the dynamics and formation of XPR in these hybrid plasmas. The discharge #195280 is used as the modeling reference to provide real EFIT equilibrium and other experimental settings. Anomalous cross-field transport coefficients are iteratively calculated based on experimentally measured electron temperature and density profiles at the outer midplane. In additional, all particle drifts ($E \times B$, $B \times \nabla B$), as well as associated currents are included in the modeling to access the role of drifts in the formation of an XPR. As in the experiments, strong seeding of N_2 is set from both the private flux and common flux region. The seeding rate in the modeling is scanned from $1 \times 10^{20}/\mathrm{s}$ to $5.5 \times 10^{20}/\mathrm{s}$ until complete detachment is achieved.

For the first time in DIII-D, SOLPS-ITER was able to qualitatively reproduce the divertor conditions and radiation patterns towards the formation of an XPR observed in experiments. The bottom of Figure 1 shows the evolution of the total radiation extracted from SOLPS-ITER modeling with increased N_2 seeding rate. The radiation pattern evolves from attached state (outer target) to the formation of an XPR. In the attached state, the peak radiation is along the inner divertor leg and near the outer target. As the seeding rate of N_2 increases, the radiation zone moves away from the outer target towards the X-point and eventually above the X-point. With the formation of an XPR, plasma accumulates at the LFS separatrix and the electron temperature near the X-point quickly drops to below 5eV, as shown in figure 2(a) and 2(b). Both the radiation and ionization are mainly concentrated in the confined region. The volumetric recombination is significantly reduced in the LFS area along the separatrix. With an XPR, over 90% of the power from upstream is dissipated in the radiating and ionizing region above the X-point.

The right of figure 2 shows the evolution of electron temperature, neutral density, total plasma pressure at the X-point, and the pedestal temperature as functions of the N_2 seeding rate. The electron temperature at the X-point decreases continuously with increased N_2 seeding. With strong N_2 puffing, i.e. N_2 seeding rate $>4.7\times 10^{20}/s$, the divertor region become more transparent for the recycling neutrals so that the neutral density at the X-point is significantly increased. With ionization and charge exchange collision of neutrals, the X-point region becomes cooler and the plasma pressure drops sharply. In the meantime, the pedestal temperature is decreased around 40%, as in experiments. As the puffing rate of N_2 increases above $5.5\times 10^{20}/s$, a radiation collapse was found in the simulations. Similar phenomena were reported in the XPR modeling in ASDEX Upgrade [2]. In the experiment, over-gassing of impurity could lead to the formation of the unstable MARFEs and disruptions.

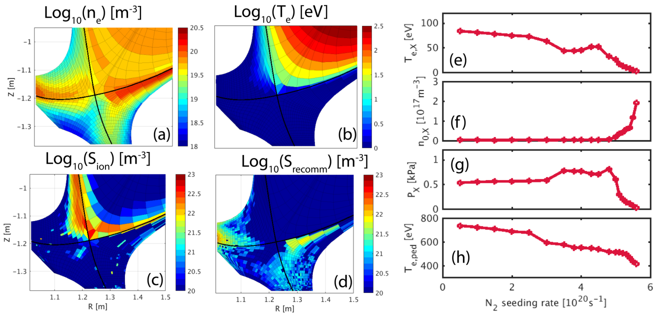

Fig. 2. *Left: cross sections of (a) n_e, (b) T_e, (c) ion source S_{ion} from ionization and (d) ion sink S_{recom} from volume recombination with an XPR. Right: evolution of (e) T_e, (f) neutral density, (g) total plasma pressure at the X-point, and (h) pedestal T_e with a scan of the N_2 seeding rate.*

Drifts are found to play an essential role in the formation of an XPR. With ion $B\times\nabla B$ drift towards the X-point, the $E\times B$ drifts push the particles from the outer common flux region through the private flux region to the inner common flux region, resulting in a partially detached inner divertor, as shown in figure 1. As the N_2 seeding rate increases, the radiation peak in the HFS moves towards the X-point quicker than that in the LFS. In the shallow and deep XPR states, strong radial temperature gradient across the separatrix near the X-point shown in figure 2(b) leads to large radial electric field and strong poloidal $E\times B$ flow from the HFS to the LFS. Consequentially, the radiation peaks towards the LFS, which is consistent with the experimental observations. Similarly in the modeling of XPR regime in AUG, larger $E\times B$ flows give major contribution to the net particle flows and change the impurity flow pattern completely.

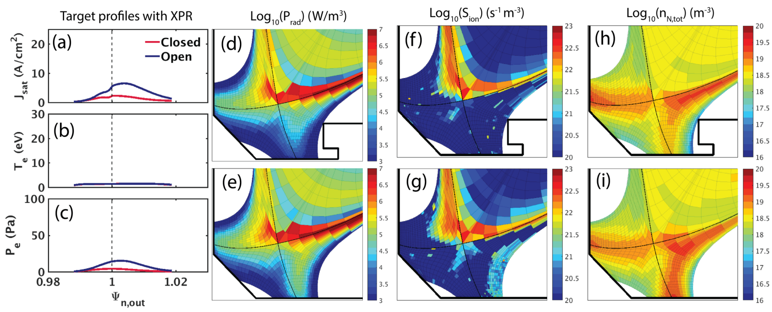

Fig. 3. *(a-c): Comparisons of J_{sat}, T_e and P_e profiles along the outer target with XPR in the closed (red) and open (blue) divertor configurations. Comparisons of the cross sections of (d-e) P_{rad}, (f-g) S_{ion} and (h-i) total nitrogen density in the closed (upper) and open (lower) configurations.*

SOLPS-ITER also predicts that in an open divertor configuration without pumping, even when the radiation front moves above the X-point (figure 3(e)), complete detachment is not achieved. With the formation of an XPR, the target temperature drops below 2eV quickly, but there is still substantial ion flux to the target, as shown in figure 3(a) and 3(b). This is consistent with the XPR experiment with the outer strike point at the lower shelf of DIII-D. Compared to the results in a more closed divertor, SOLPS-ITER indicates stronger ionization source (figure 3(g)) and higher N_2 density (figure 3(i)) in the open divertor region due to the absence of pumping for particle control. Further SOLPS simulations find that the open divertor with pump on could reduce the divertor particle flux and achieve complete detachment similar as that in a closed divertor.

In conclusion, The XPR is an attractive scenario that may contribute to solving the power exhaust challenges in future fusion devices. First ever 2D boundary simulations of an XPR in DIII-D further fill the gaps between the experiments and theoretical analysis, providing a better understanding of the operation window and access condition of XPR. Further integration of a high-performance core with advanced power exhaust scenarios such as XPR can provide important references for the operation and design of an FPP.

ACKNOWLEDGEMENTS

This work was supported by US DOE under DE-FC02-04ER54698

REFERENCES

[1] Bernert M. *et al* 2017 *Nucl. Mater. Energy* **12** 111
[2] I Yu Senichenkov *et al* 2021 *Plasma Phys. Control. Fusion* **63** 055011